Received: 13 July 2020 | Revised: 15 October 2020 | Accepted: 30 October 2020

DOI: 10.1002/er.6213

SPECIAL ISSUE RESEARCH ARTICLE

INTERNATIONAL JOURNAL OF ENERGY RESEARCH WILEY

Synergistic enhancement of CdSe/ZnS quantum dot and liquid scintillator for radioluminescent nuclear batteries

Zhiheng Xu[1,2] | **Zhengrong Zhang**[1] | **Kelum A. A. Gamage**[3] | **Yunpeng Liu**[1,2] | **Huangfeng Ye**[1] | **Xiaobin Tang**[1,2]

[1]Department of Nuclear Science and Technology, Nanjing University of Aeronautics and Astronautics, Nanjing, China

[2]Key Laboratory of Nuclear Technology Application and Radiation Protection in Astronautics (Nanjing University of Aeronautics and Astronautics), Ministry of Industry and Information Technology, Nanjing, China

[3]Electronics & Electrical Engineering, James Watt School of Engineering, University of Glasgow, Glasgow, UK

Correspondence
Xiaobin Tang, Department of Nuclear Science and Technology, Nanjing University of Aeronautics and Astronautics, Nanjing 210016, China.
Email: tangxiaobin@nuaa.edu.cn

Funding information
China Postdoctoral Science Foundation, Grant/Award Number: 2019M661836; National Natural Science Foundation of China, Grant/Award Numbers: 11675076, 12005101; the Fundamental Research Funds for the Central Universities, Grant/Award Number: NP2018462

Summary

The feasibility of utilizing CdSe/ZnS quantum dots (QDs) in liquid scintillator radioluminescent nuclear batteries to improve battery performance was studied. The peak position of the radioluminescence emission spectra of liquid scintillator can be regulated by controlling the QD components. This method is suitable for obtaining a satisfactory spectral matching between fluorescence materials and photovoltaic devices to increase the output performance of the battery. In the experiment, CdSe/ZnS QDs were introduced into Emulsifier-Safe liquid scintillator, and the output properties of radioluminescent nuclear batteries were investigated via X-ray. Results indicate that the battery with 15 mg CdSe/ZnS QDs generated the best electric power under different tube voltages. To analyze the X-ray radioluminescence effects of the liquid scintillator, the radioluminescence spectra of the Emulsifier-Safe with and without CdSe/ZnS QDs were measured and compared. The spectral matching degree between the Emulsifier-Safe with different concentrations of CdSe/ZnS QDs and the GaAs device was also analyzed by considering luminescence utilization in batteries. This framework can serve as a guide for the development of a radioluminescent material system for long-lasting, high-performance power supplies.

KEYWORDS

energy conversion, liquid scintillator, nuclear battery, quantum dot

1 | INTRODUCTION

Nuclear batteries have great application prospects in space exploration, seabed monitoring and portable electronic equipment due to their advantages of high energy density, long life, strong environmental adaptability, and a wide selection of materials.[1,2] As a representative of particle-transduced nuclear batteries, radioluminescent nuclear battery is proposed and developed based on a mature and thorough study of radiovoltaic nuclear battery techniques.[3-5] The main difference between the radioluminescent and radiovoltaic nuclear batteries lies in the former adds an intermediate energy conversion process, whereas the integrated battery structure adds a fluorescence material.[6-8] The entire energy conversion process of radioluminescent nuclear battery is from nuclear energy to light energy, which is then reconverted into electrical energy, which mainly includes the radioluminescence (RL) effect and photovoltaic (PV) effect.[5] The scintillator material can convert high-energy

Zhiheng Xu and Zhengrong Zhang contributed equally to this work.

radiation particles into low-energy visible light, and then combined with energy conversion technology can achieve electrical energy supply and reduce the radiation damage effect of PV devices.[9,10] Different types of radiation particles can be considered as the excitation sources of nuclear batteries, among which X-ray has strong penetrating ability and weak radiation damage effect on devices.[11-14] X-ray-based long-life self-powered technology has broad application prospects in many fields such as radiation safety testing, communication sensing, and high-energy physics research, especially for the special needs of deep space exploration.[15,16]

As one kind of mature fluorescence materials, liquid scintillators are directly sensitive to X-rays or gamma radiation and can be used to change the spectral wavelength of the rays to the region of visible light.[17,18] Furthermore, liquid scintillators are organic scintillators with high luminous efficiency and are characterized by their low price, adequate attenuation length, long stability (with careful chemical treatment), good plasticity, and inherent radiation resistance.[19,20] Liquid scintillation can effectively absorb X-rays, enhance the efficiency of ray capture, and improve the RL response through inelastic scattering. Given these characteristics, liquid scintillators are promising candidates for intermediate energy conversion materials in X-ray nuclear batteries. However, the matching between the liquid scintillators and the PV device is not highly satisfactory. As a new type of luminescent materials, quantum dots (QDs) have the characteristics of high fluorescence quantum efficiency, high carrier mobility, adjustable emission wavelength, and good emission stability.[21-23] The Stokes shift of QDs can effectively regulate the emission wavelength of RL. Therefore, QDs were introduced into liquid scintillator to regulate the emission spectrum and match the peak of the external quantum efficiency (EQE) curve of the PV device.[24-26] This process provides a feasible candidate for effectively improving battery performance.[27,28] And as of now, nuclear batteries based on liquid scintillators doped with QDs have been rarely reported. The characteristics of X-ray radioluminescent nuclear batteries based on Emulsifier-Safe liquid scintillator with and without CdSe/ZnS QDs under various X-ray intensities were investigated.

The battery structure proposed by this research is shown in Figure 1, which includes three parts: X-ray emitter, liquid scintillator doped with QDs, and GaAs device. The liquid scintillator absorbs X-ray energy and produces RL (about 420 nm blue-violet light). CdSe/ZnS QDs in liquid scintillator can convert the blue-violet light to the longer wavelength luminescence, which can effectively generate electron-hole pairs in the GaAs PV device, and separate and aggregate to the two ends under the action of the built-in electric field to form a potential difference. Finally, the battery delivers an output current after being connected to an external circuit. In this work, we explored the effects of CdSe/ZnS QDs and liquid scintillators on the modulation and enhancement of fluorescence, and performed performance analysis based on radioluminescent nuclear batteries.

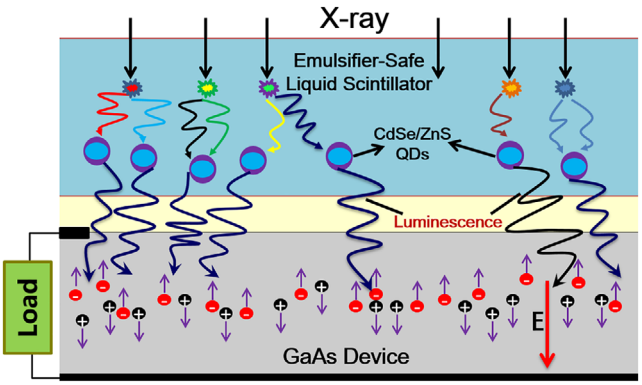

FIGURE 1 Schematic of radioluminescent nuclear battery based on X-ray, GaAs device and Emulsifier-Safe liquid scintillator doped with CdSe/ZnS QDs [Colour figure can be viewed at wileyonlinelibrary.com]

2 | MATERIALS AND METHODS

Emulsifier-Safe liquid scintillator (PerkinElmer 6 013 381, USA) was used as fluorescence material for battery due to its high flash points, good stability, and low toxicity. Fluorescence lifetime τ and quantum yield φ_f were measured by a steady-state and transient-state fluorescence spectrometer (Edinburgh Instruments FLS980, United Kingdom). τ represents the average time when particles exist in an excited state, which is related to the type of scintillator, activator of the scintillator, concentration of the wavelength shifter, and temperature. φ_f can be calculated using the following formula:

$$\varphi_f = \frac{K_f}{K_f + \sum K_i} \quad (1)$$

where K_f is the rate constant of fluorescence emission, and ΣK_i is the sum of the rate constants for non-radiative transitions such as intersystem crossings. Under the ultraviolet light excitation of 400 nm, Emulsifier-Safe possessed fluorescence lifetime τ of 1.7 ns and fluorescence quantum yield φ_f of 96.5%.

Based on the hot injection method, CdSe/ZnS QDs were prepared by reacting cadmium oxide (CdO), selenium (Se), zinc acetate dihydrate ($C_4H_{10}O_6Zn$), and

sodium sulphide ($Na_2S{\cdot}9H_2O$) in octadecylene solution. The optical properties of the fluorescent material were obtained by a Cary Eclipse fluorescence spectrophotometer (Agilent Technologies G9800a, Malaysia) and a UV/Vis spectrophotometer (Shimadzu UV-2550, Japan). As shown in Figure 2, the excitation and emission peak wavelength of Emulsifier-Safe are approximately 396 and 420 nm, and the emission peak wavelength of CdSe/ZnS QDs is approximately 520 nm.

The excitation source used for the measurement of the RL emission spectra of these fluorescent materials is X-rays. A 50 W Mo X-ray tube (Shanghai KeyWay Electron Company Ltd. KYW900A, China) was used as a suitable substitute for the low-energy X-ray source due to safety concerns and convenience. The X-ray tube was operated with tube voltage U of 30 to 50 kV and tube current I of 800 μA. The tube voltage was adjusted so that the accelerated electrons can obtain the X-ray with different average energy levels. The basic specifications of the X-ray tube are listed in Table S1. X-ray energy spectra were obtained by a silicon drift detector (AMPTEK X-123, USA) under the excitation condition of 30 to 50 kV tube voltage (Figure 3).

3 | RESULTS AND DISCUSSION

3.1 | Optical properties of liquid luminescent materials

Different amounts (0-20 mg) of CdSe/ZnS QDs powder were added to the same volume (8 mL) of Emulsifier-Safe liquid scintillation solution to discuss their RL properties. The mixture was then placed in an ultrasonic disperser for about 5 minutes to distribute evenly QDs powder. Under the chosen X-ray tube (tube voltage: 30, 35, 40, 45, and 50 kV; tube current: 800 μA) excitation, the patterns of the RL emission spectra of the Emulsifier-Safe doped with 0, 1, 2, 3, 4, 5, 10, 15, and 20 mg of CdSe/ZnS QDs are also constantly changing, as shown in Figure 4. Before the addition of CdSe/ZnS QDs, the emission peak wavelength of the pure Emulsifier-Safe has only one main peak at about 420 nm. With the gradual addition of QDs, a new and stronger main peak appeared at approximately 520 nm in the mixture. As more and more QDs were dissolved in Emulsifier-Safe liquid scintillator, the color of the mixture turned from blue to blue-green then to a deep, steady yellow-green. The spectral curve also shows a changing trend one after another. The relative luminescence intensities at 520 nm increased significantly with the increasing amount of CdSe/ZnS QDs. Conversely, the RL relative intensities at 420 nm decreased with the increasing QDs. As the amount of CdSe/ZnS QDs in the mixed liquid increases, the QDs can absorb more RL from the liquid scintillator. The photoluminescence relative intensities at 520 nm reached the maximum when 20 mg of CdSe/ZnS QDs were completely dissolved in 8 mL of Emulsifier-Safe liquid scintillator. The added QDs serve a dual function, which can not only effectively transfer the RL peak wavelength of the liquid scintillation, and also efficiently absorb fluorescent photons and improve the overall luminescence emission intensity.[29-31] Moreover, the relative RL intensity of the Emulsifier-Safe was enhanced with increasing tube voltage, but the peak wavelengths remained steady and unchanged.

It is worth noting that in this process, the amount of QDs should also be controlled. Comparing before and

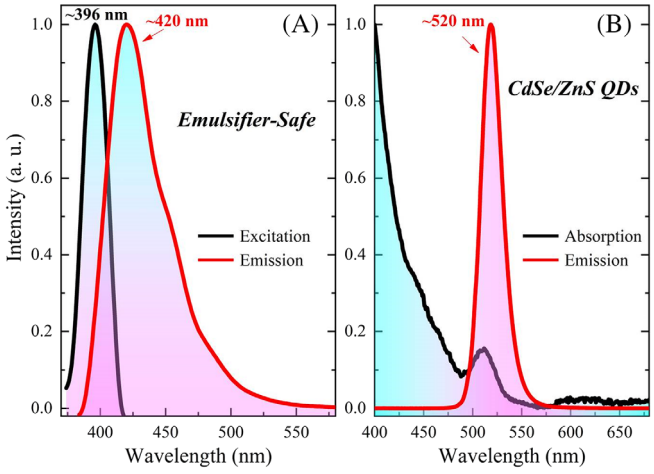

FIGURE 2 Optical spectra of (A) Emulsifier-Safe and (B) CdSe/ZnS QDs [Colour figure can be viewed at wileyonlinelibrary.com]

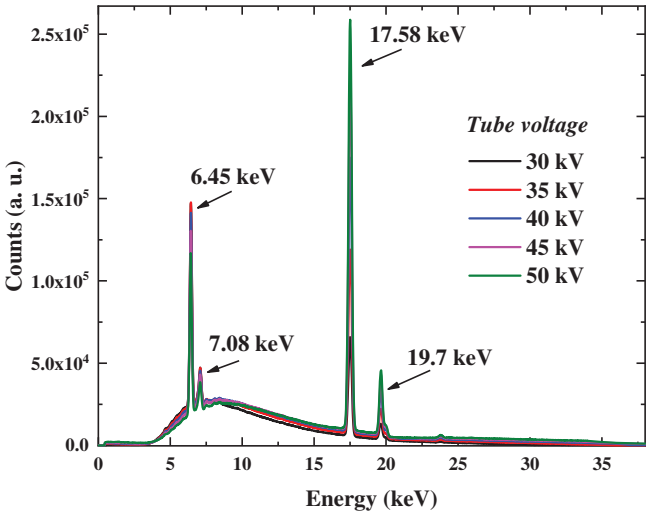

FIGURE 3 X-ray energy spectra for a tube voltage of 30 to 50 kV [Colour figure can be viewed at wileyonlinelibrary.com]

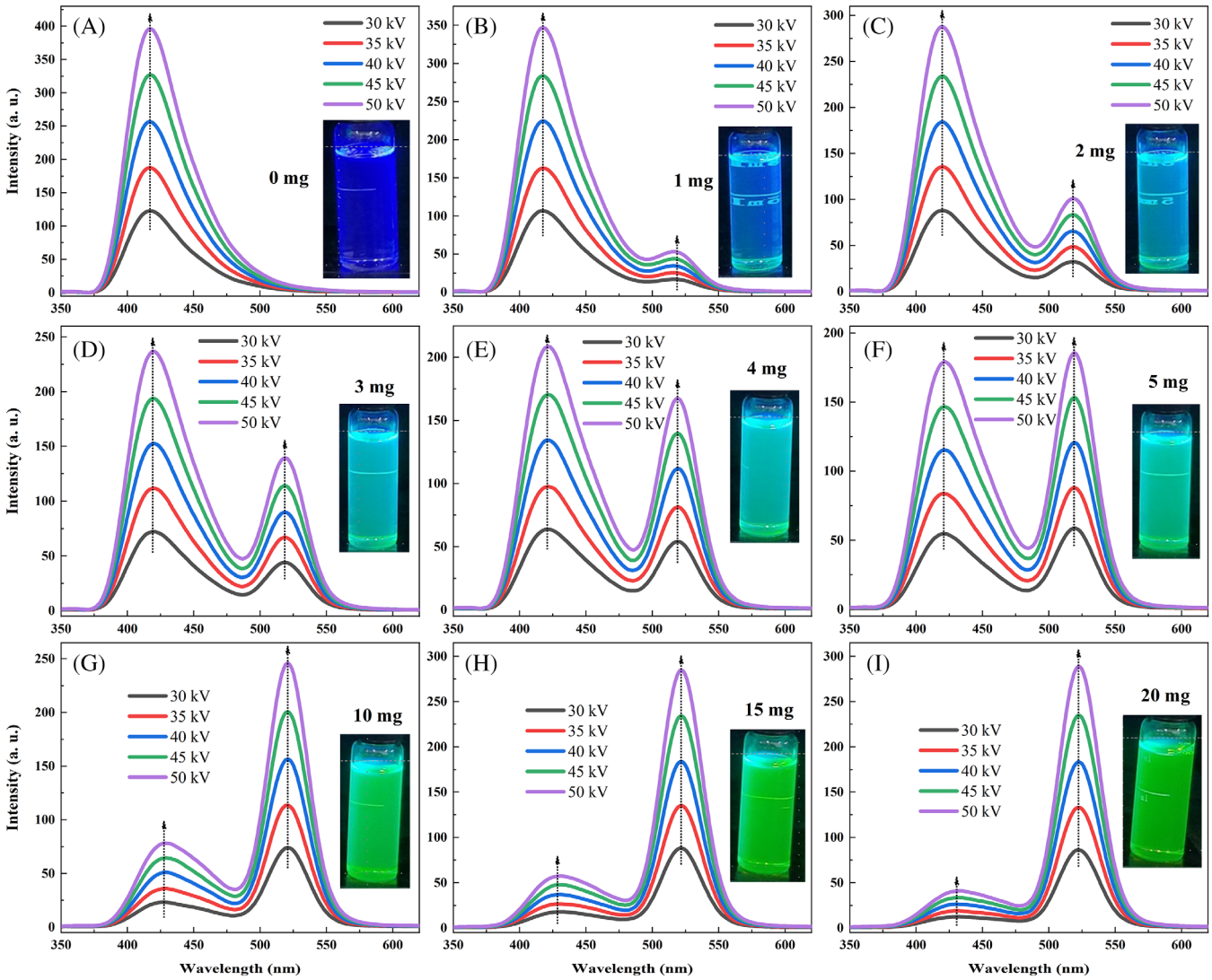

FIGURE 4 RL emission spectra of Emulsifier-Safe doped with (A) 0, (B) 1, (C) 2, (D) 3, (E) 4, (F) 5, (G) 10, (H) 15, and (I) 20 mg CdSe/ZnS QDs. Illustrations are the pictures of these experimental samples illuminated by 365 nm ultraviolet light [Colour figure can be viewed at wileyonlinelibrary.com]

after adding a certain amount of QDs, the peak emission wavelength of these mixed samples has effectively shifted, but the overall relative RL intensity has also decreased to a certain extent. Although the more the amount of QDs, the stronger the light absorption, but it will also reduce the transmission of the fluorescent material (Figure 5). The absorbance (A) and transmittance (T) can be expressed as follows:

$$A = \lg(1/T) = \lg(I_0/I_t) \quad (2)$$

where I_0 is the intensity of incident light, and I_t is the intensity of transmitted light. The transmittance of the mixed liquor decreases with the increase of QDs amount. A series of troughs at 490 to 530 nm was observed in the transmittance curves after the addition of CdSe/ZnS QDs in the liquid scintillator. The transmittance decreased by about 25% at around 515 nm, when the QDs amount increased from 10 mg to 20 mg. As the content of QDs in the mixed liquid increases, the RL intensity at the peak emission wavelength of the liquid scintillation at 420 nm gradually decreases, and at the same time, the turbidity of the solution also increases, the self-absorption effect is stronger, and the intensity at the peak wavelength of 520 nm also decreases. Therefore, the luminescence intensity of the mixed liquid was weakened by the high density of CdSe/ZnS QDs in the liquid scintillator.

Figure 6 reflects the RL test result pictures of Emulsifier-Safe doped with 0, 15, and 20 mg of CdSe/ZnS QDs. The closer to the X-ray emission port, the stronger the intensity of the RL. As the tube voltage increases, the X-ray field and range also gradually

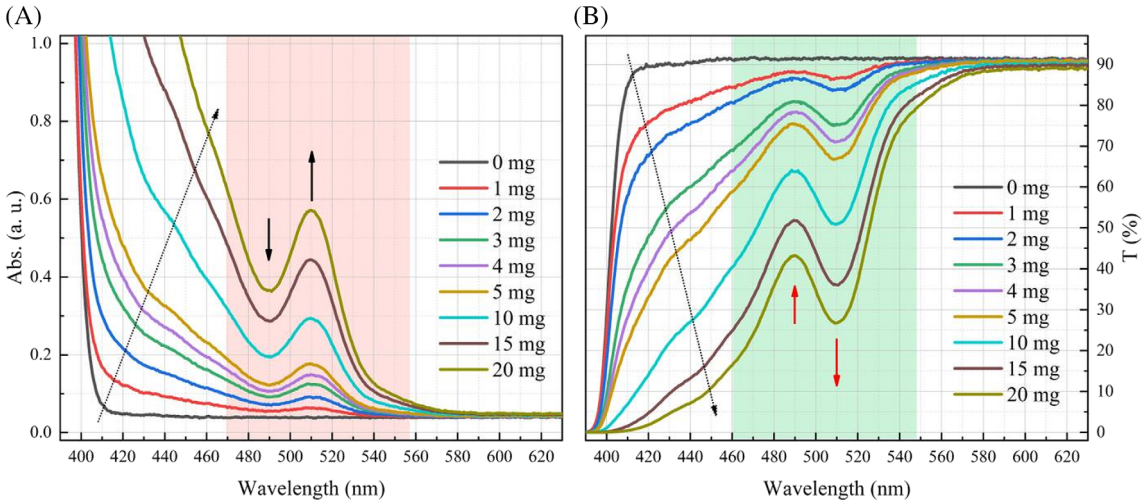

FIGURE 5 (A) Absorption and (B) transmission spectra of the Emulsifier-Safe liquid scintillator doped with different amounts (0, 1, 2, 3, 4, 5, 10, 15, and 20 mg) of CdSe/ZnS QDs [Colour figure can be viewed at wileyonlinelibrary.com]

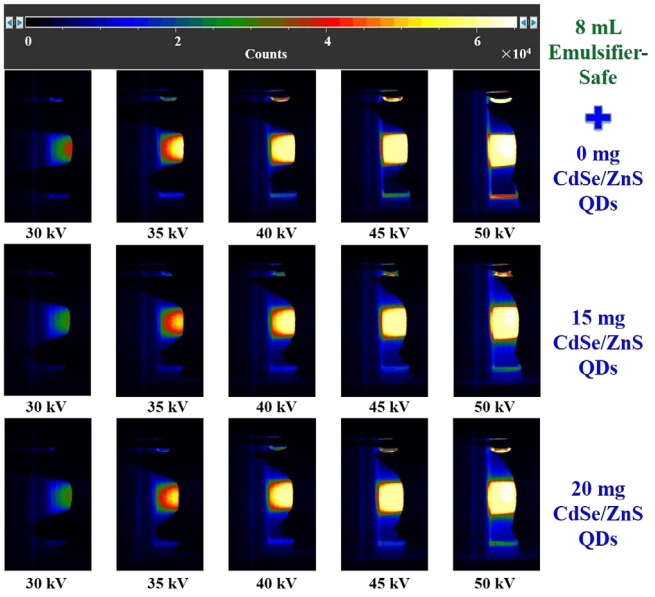

FIGURE 6 Images of Emulsifier-Safe doped with 0, 15, and 20 mg CdSe/ZnS QDs under different X-ray parameters (tube voltage: 30, 35, 40, 45, and 50 kV; tube current: 800 μA) excitation were taken by EMCCD camera [Colour figure can be viewed at wileyonlinelibrary.com]

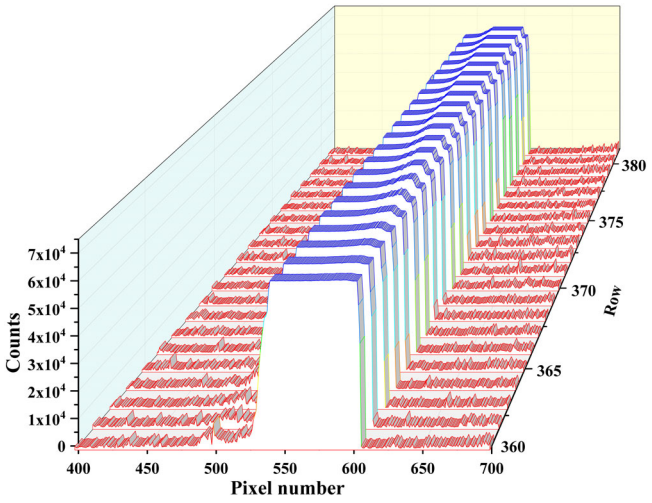

FIGURE 7 Counting statistics of RL images of Emulsifier-Safe taken by EMCCD camera under 50 kV tube voltage [Colour figure can be viewed at wileyonlinelibrary.com]

expand. Moreover, the luminescence intensities increased significantly with increasing tube voltage and reached the maximum at tube voltages as high as 50 kV, as well as the other cases (Emulsifier-Safe doped with 1, 2, 3, 4, 5, and 10 mg of CdSe/ZnS QDs). Figure 7 shows the photon count statistics of Emulsifier-Safe on the horizontal plane under the excitation condition of 50 kV tube voltage, based on the results of multiple measurements by the camera.

3.2 | Spectral coupling and matching analysis

GaAs device was used as the photoelectric converter of radioluminescent nuclear battery due to direct bandgap, large light absorption coefficient, wide bandgap, low leakage currents, high radiation resistance, and a series of advantages.[32-34] The spectral response of the GaAs device to the fluorescent material is shown in Figure 8. But before adding CdSe/ZnS QDs, when there is only Emulsifier-Safe, the emitted RL was mainly concentrated in the low response section. As the amount of QDs increases, the peak wavelength was red-shifted, and the

luminous intensity gradually increased, as well as the proportion in the high response interval of the GaAs device. The higher the amount of QDs in the liquid scintillation system, the more the peak wavelength of the RL emission shifts from 420 to 520 nm, which is also more conducive to the absorption application of GaAs device (normalized EQE can be as high as 90% ~ 97.5%). Even though the overall RL intensity was lost to some extent after mixing the Emulsifier-Safe and CdSe/ZnS QDs, the photoelectric response capacity of the adjusted RL emission spectra under the GaAs devices were greatly improved.

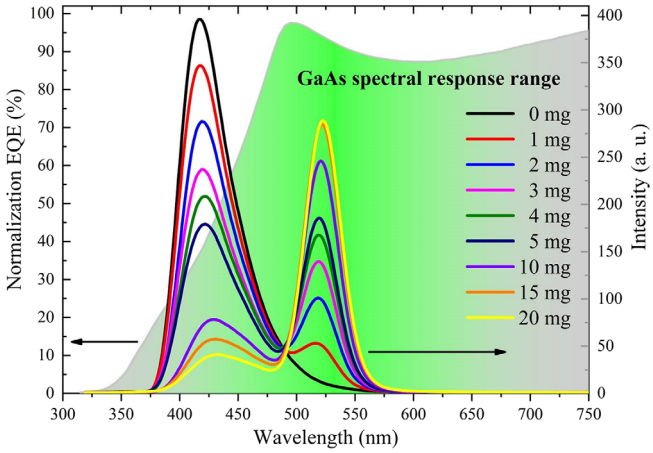

FIGURE 8 Normalized EQE of the GaAs device and RL emission spectra of Emulsifier-Safe doped with CdSe/ZnS QDs under excitation of 50 kV tube voltage and 800 μA tube current [Colour figure can be viewed at wileyonlinelibrary.com]

3.3 | Electrical performance of liquid nuclear battery

The *I-V* characteristic curves of radioluminescent nuclear batteries were measured by a dual-channel system source-meter instrument (Keithley Model 2636A, USA) at room temperature. Figure 9 shows the changes in electrical properties of the batteries at different tube voltages as a function of CdSe/ZnS QDs amount (0-20 mg).

Under the excitation of a specific tube voltage, with the increase of the QDs amount, the short-circuit current (I_{sc}) and maximum output power (P_{max}) gradually increased and reached saturation, but although the values of the open-circuit voltage (V_{oc}) and fill factor (FF) fluctuate, the overall change was not large. As the tube voltage increases, the performance optimization effect is more obvious. However, there are also competitions and trade-offs in this process. After adding about 15 mg of CdSe/ZnS QDs, the effect of spectrum adjustment can make the battery output power reach a better

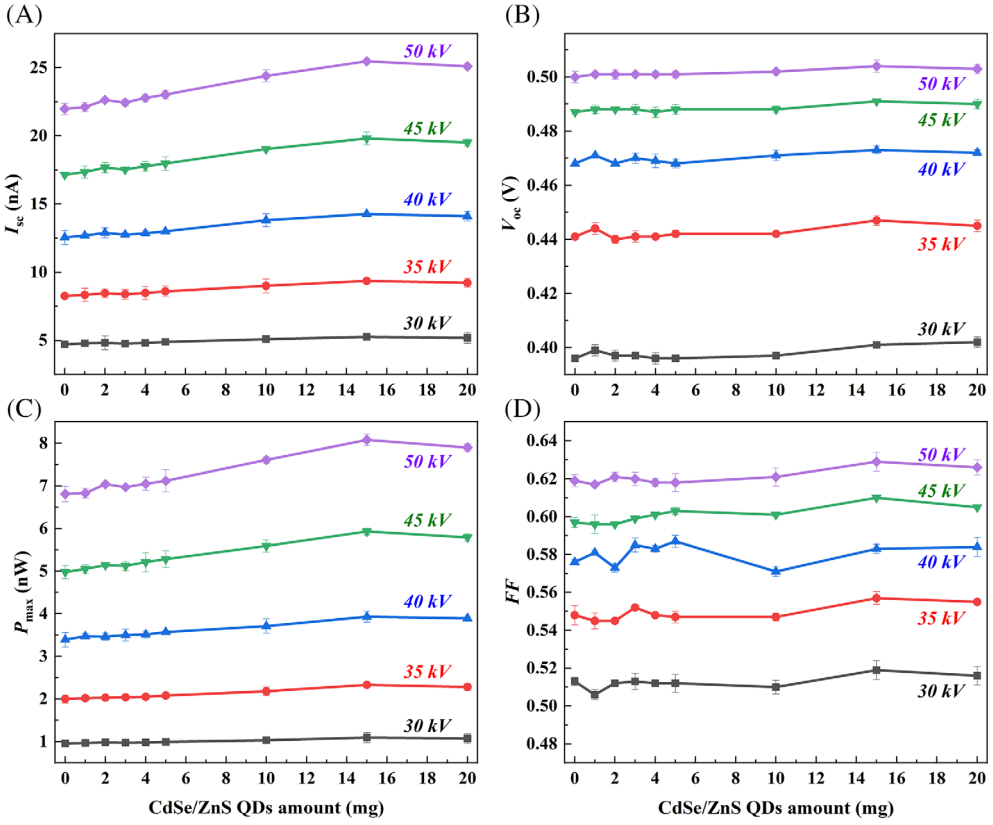

FIGURE 9 Electrical properties of the batteries at different tube voltages as a function of CdSe/ZnS QDs amount: (A) I_{sc}, (B) V_{oc}, (C) P_{max}, and (D) *FF*. The tube current remained unchanged at 800 μA [Colour figure can be viewed at wileyonlinelibrary.com]

value. The output performance of the battery with 20 mg of QDs is lower than that with 15 mg. This is mainly because the amount of QDs continues to increase, the light transmittance of the mixed liquid gradually decreases, but the increase in light intensity value is not large enough. Moreover, the luminescence intensity at 520 nm is almost similar for 15 and 20 mg of QDs, but the luminescence intensity for 20 mg of QDs is less than that for 15 mg at 420 nm. From the above optical and electrical performance test results, it can be seen that under the experimental conditions when the amount of QDs added is about 15 mg, it is relatively advantageous in a comprehensive contest of all parties. Therefore, it can be known that optimizing the coupling response between energy conversion components in the radioluminescent nuclear battery can effectively improve its overall output performance.

4 | CONCLUSIONS

The liquid scintillator radioluminescent nuclear battery enhanced by CdSe/ZnS QDs was demonstrated by using an X-ray tube to be equivalent to a series of low-energy X-ray sources. The RL intensity at 520 nm increased significantly with increasing CdSe/ZnS QDs in Emulsifier-Safe under the same excitation condition. As the proportion of QDs in the mixed solution increases, the corresponding transmittance gradually decreases, and the degree of spectral coupling response between the fluorescent material and GaAs device is also enhanced. As a consequence, when 15 mg CdSe/ZnS QDs are added, the P_{max} of the battery is increased by 19.19% compared with the Emulsifier-Safe liquid scintillator only, under the excitation of X-ray at 45 kV tube voltage and 800 μA tube current. Based on liquid scintillation, QD doping is used to control the emission wavelength, thereby improving the coupling and matching of the spectrum, improving energy utilization, and optimizing the performance of the nuclear battery. The synergistic enhancement effect and energy conversion technology can also be effectively applied to more fields of optical detection and sensing.

ACKNOWLEDGEMENTS

This research was supported by the National Natural Science Foundation of China (Grant Nos. 12005101 and 11675076); the Project supported by China Postdoctoral Science Foundation (Grant No. 2019 M661836); the Fundamental Research Funds for the Central Universities (Grant No. NP2018462).

CONFLICT OF INTEREST

The authors declare no conflicts of interest.

SUPPLEMENTARY MATERIAL

See supplementary material for more information about the optical properties of Emulsifier-Safe liquid scintillator, the microscopic characterization of CdSe/ZnS QDs, and experimental materials and test devices.

DATA AVAILABILITY STATEMENT

The data that support the findings of this study are available on request from the corresponding author. The data are not publicly available due to privacy or ethical restrictions.

ORCID

Xiaobin Tang https://orcid.org/0000-0003-3308-0468

REFERENCES

1. Prelas MA, Weaver CL, Watermann ML, Lukosi ED, Schott RJ, Wisniewski DA. A review of nuclear batteries. *Prog Nucl Energy*. 2014;75:117-148.
2. Russo J, Litz MS, William Ray II, et al. Planar and textured surface optimization for a tritium-based betavoltaic nuclear battery. *Int J Energy Res*. 2019;43(9):4370-4389.
3. Sharma A, Melancon JM, Bailey SG, Zivanovic SR. Betavoltaic cells using P3HT semiconductive conjugated polymer. *IEEE Trans Electron Dev*. 2015;62:2320-2326.
4. Borisyuk PV, Yakovlev VP, Vasiliev OS, et al. Size-ordered ^{63}Ni nanocluster film as a betavoltaic battery unit. *Appl Phys Lett*. 2018;112:143105.
5. Xu ZH, Liu YP, Zhang ZR, et al. Enhanced radioluminescent nuclear battery by optimizing structural design of the phosphor layer. *Int J Energy Res*. 2018;42(4):1729-1737.
6. Bower KE, Barbanel YA, Shreter YG, Bohnert GW. *Polymers, Phosphors, and Voltaics for Radioisotope Microbatteries*. Boca Raton, FL: CRC Press; 2002.
7. Lu M, Zhang GG, Fu K, Yu GH, Su D, Hu JF. Gallium nitride schottky betavoltaic nuclear batteries. *Energy Convers Manag*. 2011;52(4):1955-1958.
8. Liu YP, Tang XB, Xu ZH, Hong L, Wang P, Chen D. Optimization and temperature effects on sandwich betavoltaic microbattery. *Sci China Technol Sci*. 2014;57(1):14-18.
9. Zhang ZR, Liu YP, Tang XB, et al. GaAs low-energy X-ray radioluminescence nuclear battery. *Nucl Instrum Methods Phys Res B*. 2018;415:9-16.
10. Yu DJ, Wang P, Cao F, et al. Two-dimensional halide perovskite as β-ray scintillator for nuclear radiation monitoring. *Nat Commun*. 2020;11(1):1-10.
11. Artun O. A study of nuclear structure for ^{244}Cm, ^{241}Am, ^{238}Pu, ^{210}Po, ^{147}Pm, ^{137}Cs, ^{90}Sr and ^{63}Ni nuclei used in nuclear battery. *Mod Phys Lett A*. 2017;32(22):1750117.
12. Butera S, Whitaker MDC, Lioliou G, Barnett AM. AlGaAs ^{55}Fe X-ray radioisotope microbattery. *Sci Rep*. 2016;6(1):38409.
13. Butera S, Lioliou G, Krysa AB, Barnett AM. $Al_{0.52}In_{0.48}P$ ^{55}Fe X-ray-photovoltaic battery. *J Phys D Appl Phys*. 2016;49(35):355601.
14. Lioliou G, Meng X, Ng JS, Barnett AM. Temperature dependent characterization of gallium arsenide X-ray mesa pin photodiodes. *J Appl Phys*. 2016;119(12):124507.

15. Wei HT, Fang YJ, Mulligan P, et al. Sensitive X-ray detectors made of methylammonium lead tribromide perovskite single crystals. *Nat Photon*. 2016;10(5):333-339.
16. Walton R, Anthony C, Ward M, Metje N, Chapman DN. Radioisotopic battery and capacitor system for powering wireless sensor networks. *Sensor Actuat A Phys*. 2013;203:405-412.
17. Xu ZH, Jin ZG, Tang XB, et al. Designing performance enhanced nuclear battery based on the cd-109 radioactive source. *Int J Energy Res*. 2020;44(1):508-517.
18. Chen QS, Wu J, Ou XY, et al. All-inorganic perovskite nanocrystal scintillators. *Nature*. 2018;561(7721):88-93.
19. Swiderski L, Moszyński M, Wolski D, et al. Suppression of gamma-ray sensitivity of liquid scintillators for neutron detection. *Nucl Instrum Methods Phys Res A*. 2011;652(1):330-333.
20. Chang Z, Okoye NC, Urffer MJ, Green AD, Childs KE, Miller LF. On the scintillation efficiency of carborane-loaded liquid scintillators for thermal neutron detection. *Nucl Instrum Methods Phys Res A*. 2015;769:112-122.
21. Pevere F, Treskow CV, Marino E, et al. X-ray radiation hardness and influence on blinking in Si and CdSe quantum dots. *Appl Phys Lett*. 2018;113(25):253103.
22. Yang DD, Li XM, Zhou WH, et al. $CsPbBr_3$ quantum dots 2.0: benzenesulfonic acid equivalent ligand awakens complete purification. *Adv Mater*. 2019;31(30):1900767.
23. Ye S, Guo JQ, Song J, Qu JL. Achieving high-resolution of 21 nm for STED nanoscopy assisted by CdSe@ZnS quantum dots. *Appl Phys Lett*. 2020;116(4):041101.
24. Litvin AP, Martynenko IV, Purcell-Milton F, Baranov AV, Fedorov AV, Gun'ko YK. Colloidal quantum dots for optoelectronics. *J Mater Chem A*. 2017;5(26):13252-13275.
25. Li XM, Cao F, Yu DJ, et al. All inorganic halide perovskites nanosystem: synthesis, structural features, optical properties and optoelectronic applications. *Small*. 2017;13(9):1603996.
26. Du ZL, Artemyev M, Wang J, Tang JG. Performance improvement strategies for quantum dot-sensitized solar cells: a review. *J Mater Chem A*. 2019;7(6):2464-2489.
27. Zhang ZR, Tang XB, Liu YP, et al. Use the indirect energy conversion of the phosphor layer to improve the performance of nuclear batteries. *Energy Technol*. 2018;6:1959-1965.
28. Xu ZH, Tang XB, Liu YP, et al. ZnS:Cu phosphor layers as energy conversion materials for nuclear batteries: a combined theoretical and experimental study of their geometric structure. *Energy Technol*. 2017;5(9):1638-1646.
29. Yang DD, Li XM, Wu Y, et al. Surface halogen compensation for robust performance enhancements of $CsPbX_3$ perovskite quantum dots. *Adv Opt Mater*. 2019;7(11):1900276.
30. Chen W, Tang XB, Liu YP, et al. Radioluminescent nuclear battery containing $CsPbBr_3$ quantum dots: application of a novel wave-shifting agent. *Int J Energy Res*. 2019;43(9):4520-4533.
31. Xu ZH, Tang XB, Liu YP, et al. $CsPbBr_3$ quantum dot films with high luminescence efficiency and irradiation stability for radioluminescent nuclear battery application. *ACS Appl Mater Interfaces*. 2019;11(15):14191-14199.
32. Chen H, Jiang L, Chen XY. Design optimization of GaAs betavoltaic batteries. *J Phys D Appl Phys*. 2011;44(21):215303.
33. Butera S, Lioliou G, Barnett AM. Gallium arsenide ^{55}Fe X-ray-photovoltaic battery. *J Appl Phys*. 2016;119:064504.
34. Spencer MG, Alam T. High power direct energy conversion by nuclear batteries. *Appl Phys Rev*. 2019;6(3):031305.

SUPPORTING INFORMATION

Additional supporting information may be found online in the Supporting Information section at the end of this article.

How to cite this article: Xu Z, Zhang Z, Gamage KAA, Liu Y, Ye H, Tang X. Synergistic enhancement of CdSe/ZnS quantum dot and liquid scintillator for radioluminescent nuclear batteries. *Int J Energy Res*. 2021;45:12195–12202. https://doi.org/10.1002/er.6213